

available at www.sciencedirect.comwww.elsevier.com/locate/matchar

Short communication

Matrix grain characterisation by electron backscattering diffraction of powder metallurgy aluminum matrix composites reinforced with MoSi_2 intermetallic particles

J. Corrochano*, P. Hidalgo, M. Lieblisch, J. Ibáñez

Physical Metallurgy Department, National Centre for Metallurgical Research, CENIM-CSIC, Avda. Gregorio del Amo 8, 28040 Madrid, Spain

ARTICLE DATA

Article history:

Received 31 May 2010

Received in revised form

2 August 2010

Accepted 27 August 2010

Keywords:

Aluminum alloys

Composite materials

Powder technology

Ball milling

Grain refinement

Electron backscatter diffraction

the brittle reinforcing particles are fragmented and become embedded in the softer aluminum matrix. EBSD has been used extensively to characterise submicrometer microstructure in monolithic deformed alloys [5,6]. However, to the authors' knowledge, EBSD has scarcely been used to investigate AMCs and there is limited information on the matrix microstructure of milled AMCs after consolidation processes such as extrusion [7–9]. In the present work, electron back-scattered diffraction (EBSD) has been used to characterise matrix grain size and grain orientation in six powder metallurgy AA6061/ MoSi_2 /15p composites and three unreinforced matrices processed with and without ball milling, followed by hot extrusion. The aim is to know the effect of milling on the matrix grain structure of extruded AMCs.

1. Introduction

The mechanical properties of particle-reinforced aluminum matrix composites (AMCs) are largely dependent on the microstructure of the materials, which in turn is largely dependent on the processing history [1]. Powder metallurgy (PM) is a commonly used processing technique for producing AMCs since it can reduce reinforcement segregation, typical of casting metallurgy processes [2]. When there is a large size difference between reinforcing and aluminum particles, high energy ball milling (BM) is used to manufacture AMCs successfully [3,4]. In the BM process, the aluminum particles are fragmented and re-welded continuously, during which

2. Experimental procedure

The starting materials were 6061 aluminum alloy powder with particle diameter $<50\ \mu\text{m}$ and two initial ranges of irregular shaped MoSi_2 particles: $<3\ \mu\text{m}$ and $10\text{--}45\ \mu\text{m}$. The AA6061 powder was blended with 15% volume of MoSi_2 particles by: wet blending, rotating cube, and planetary ball milling operating for 4 and 10 h at 200 rpm with a ratio of balls to material of 7:1. Chemical analysis was carried out on the blended powders to check the amount of Fe and O introduced during milling [3]. Fe was measured by a Varian SpectraAA 220FS atomic absorption spectrometer with an accuracy of 1%, and O by infrared absorption in a LECO TC-436 instrument as the mean value of three samples.

* Corresponding author. Tel.: +34 915538900; fax: +34 915347425.

E-mail address: javier.corrochano.flores@gmail.com (J. Corrochano).

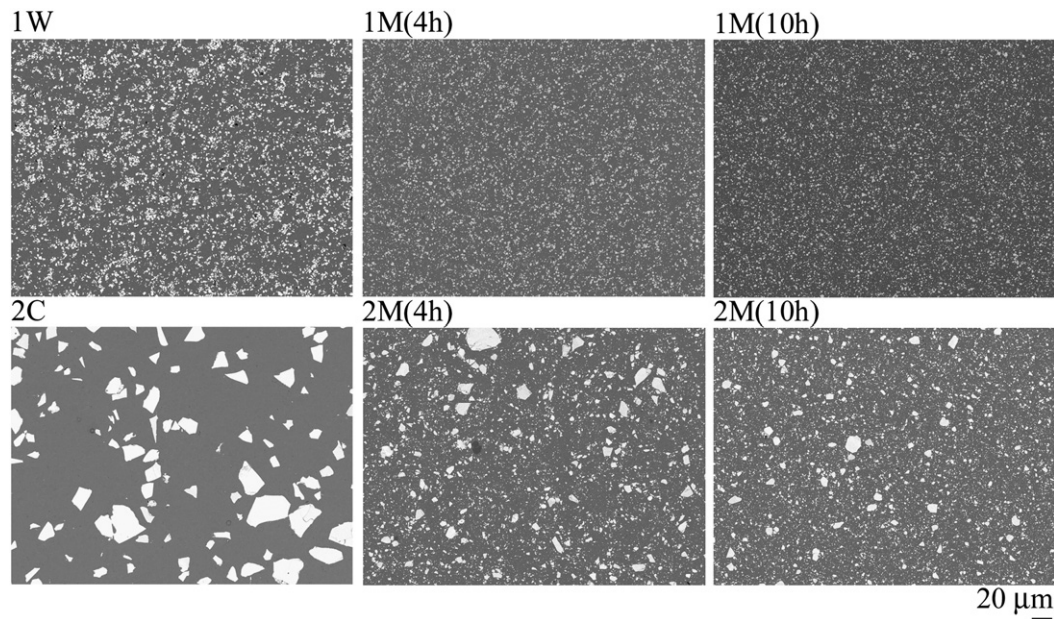


Fig. 1 – SEM micrographs of cross sections of AA6061/MoSi₂/15p composites (see Table 1 for codes).

The blends were consolidated by extrusion in a horizontal direct hot extrusion press at 450 °C. The ram speed was 0.4 mm/s and the extrusion ratio 27:1. Three monolithic 6061 Al alloy bars were also consolidated from the Al alloy powder for comparison purposes. The consolidated materials were solution heat treated at 520 °C for 0.5 h and water quenched. The solutionized bars were characterised on cross and longitudinal sections with respect to the extrusion direction by scanning electron microscopy (SEM) with a FEG-JEOL 6500 microscope and by EBSD HKL Channel 5 attached to the SEM-FEG microscope. Specimens were mechanically ground, pre-polished using 3 and 1 μm diamond pastes and finally polished using colloidal silica suspension during 30 min. Back-scattered electron SEM micrographs of composite cross sections at the same magnification are shown in Fig. 1 [3]. Qualitatively, it is seen that MoSi₂ particle size decreases with milling time and that MoSi₂ distribution is quite homogeneous, except in the wet blended composite (1W) where agglomerates can be seen.

To get the final reinforcement size in the extruded composites, portions of the extruded bars were immersed in a

solution with HCl 1:1, and particles gathered from it, filtered, cleaned and measured by image analyses with Image-Pro Plus software.

Table 1 lists the main characteristics of the processed materials. The materials were divided into three groups, according to their initial MoSi₂ particle size. As can be seen MoSi₂ particle size decreases to submicrometric level and oxygen and iron content increases in the two groups of composites as milling time increases.

Determination of matrix grain size and distribution of grain boundary misorientations was performed by EBSD HKL Channel 5 attached to a SEM-FEG-Jeol 6500SEM-FEG scanning electron microscopy. Orientation mapping was performed on a square grid with a step size of 0.2 μm for the unreinforced alloys and 0.05–0.1 μm for the composites. In order to avoid spurious boundaries, misorientations (θ) below 2° were not measured and this limit was used for all samples. Boundaries with θ between 2° and 15° were defined as low angle grain boundaries, marked by white lines, and those of θ > 15° as high angle grain boundaries (HAB), marked by black lines. The grain size was determined by the grain

Table 1 – Materials, initial MoSi₂ particle size ranges (Dr₀), median MoSi₂ particle size after blending (Dr_f), blending methods, oxygen and iron contents [3] and codes.

Material	Dr ₀ , μm	Dr _f , μm	Blending method	O, %mass	Fe, %mass (±0.01)	Code
AA6061 Group 0	–	–	As-received	0.18±0.02	0.16	0AR
		–	Ball mill: 4 h	0.4±0.1	0.20	0M(4 h)
		–	Ball mill: 10 h	0.3±0.2	0.20	0M(10 h)
AA6061/ MoSi ₂ Group 1	<3	1.4	Wet blend	0.26±0.05	0.15	1W
		0.6	Ball mill: 4 h	0.39±0.04	0.19	1M(4 h)
		0.4	Ball mill: 10 h	0.90±0.2	0.24	1M(10 h)
		17.0	Rotating cube	0.19±0.04	0.12	2C
AA6061/ MoSi ₂ Group 2	10–45	1.4	Ball mill: 4 h	0.4±0.1	0.19	2M(4 h)
		0.6	Ball mill: 10 h	0.80±0.1	0.21	2M(10 h)

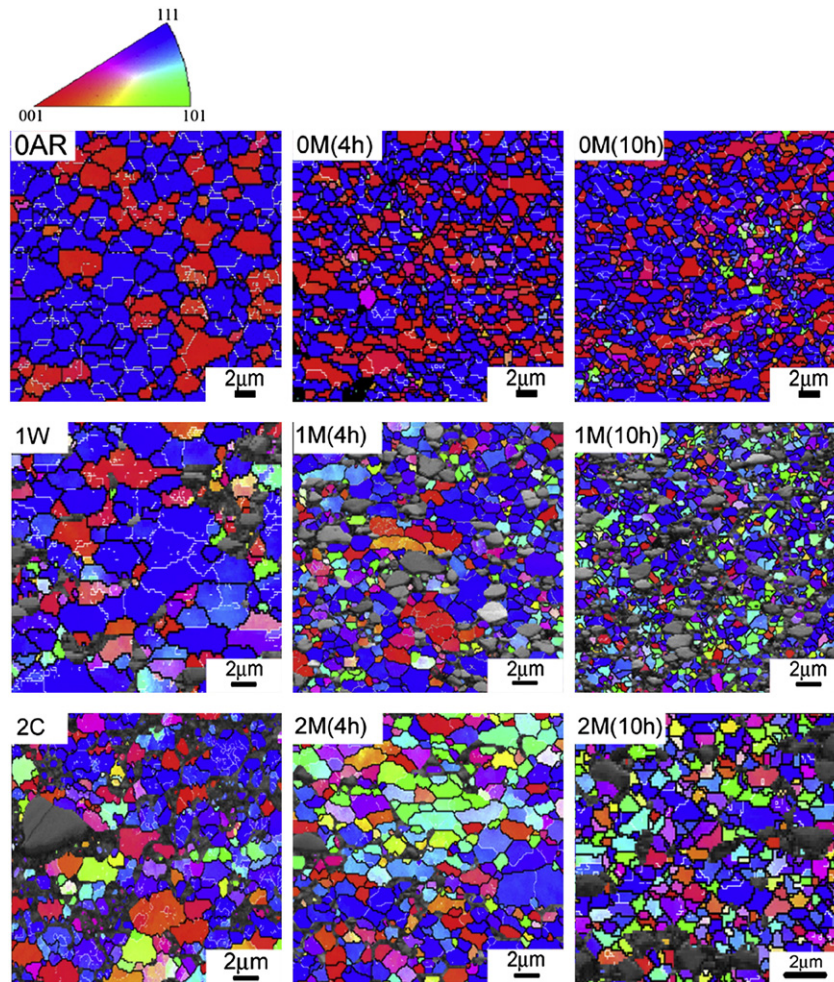


Fig. 2 – EBSD maps on cross sections of: 6061 Al, top; composites of Group 1, middle; composites of Group 2, bottom. Milling time increases from left to right (0 h, 4 h and 10 h).

reconstruction method in the EBSD maps, counting only HAB ($\theta > 15^\circ$).

3. Results and discussion

EBSD maps on cross sections of the unreinforced and composite materials are presented in Fig. 2 (note that magnifications are not the same in all the maps). A microstructure formed by (sub)grains with equiaxed morphology is observed in all cases. Measured aluminum grain size (d) and fraction of high angle boundaries (HAB%) are plotted against milling time in Fig. 3. As can be seen, matrix grain size decreases to sub-micrometric level and HAB% increases for each group of materials as milling time increases. It is noteworthy that the grain sizes of the 10 h-milled composites are of the same order as those achieved by severe plastic deformation in Al alloys [10], which proves the refinement potential of the ball milling. This refinement is attributed to the generation of dislocations due to the strong deformation occurring in the collisions between the stainless steel balls and the powders and to the pinning effect of three types of particles. These are oxide dispersoids formed during ball milling, alumina particles resulting from

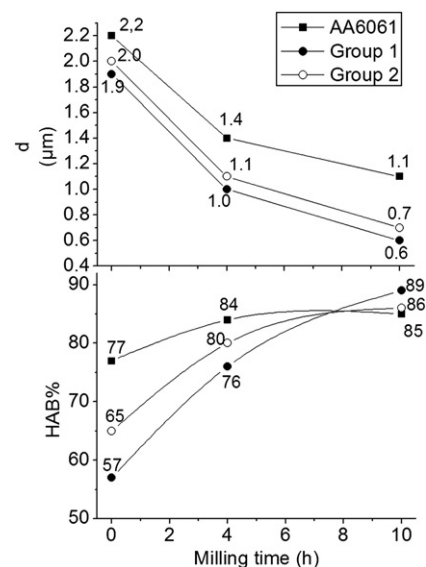


Fig. 3 – Aluminum matrix grain size (d) and fraction of high angle boundaries (HAB%) as a function of ball milling time.

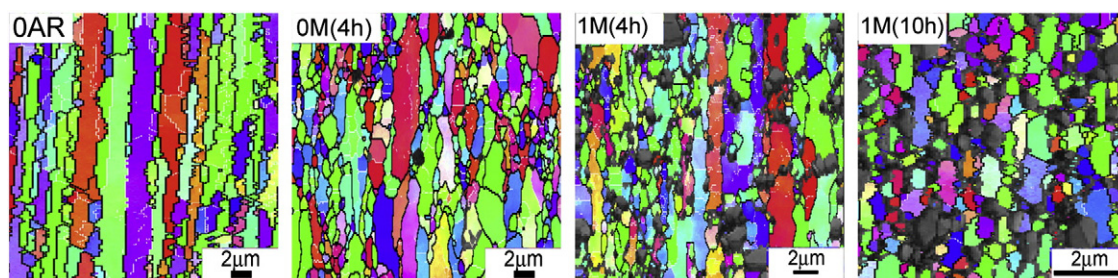


Fig. 4 – EBSD maps on longitudinal sections of, from left to right: 0AR, 0M(4 h), 1M(4 h) and 1M(10 h).

the extrusion when the alumina layer that covers the matrix particles breaks, and MoSi_2 particles under $0.5 \mu\text{m}$ [11].

In the case of the unreinforced alloys, the role of the oxide dispersoids formed during the extrusion is evident in the non-milled monolithic alloy, 0AR, where grain size is very small in comparison with those of wrought commercial alloys of similar composition (about $30 \mu\text{m}$). Furthermore, when comparing materials with the same processing, it is observed that grain size follows the order: unreinforced material > group 2 composite > group 1 composite (see codes in Table 1), which indicates that reinforcing particles also produce matrix grain refinement due to the high plastic deformation that is needed to deform the matrix around them during consolidation by extrusion.

In Fig. 4, examples of longitudinal sections corresponding to the unreinforced alloys, 0AR and 0M(4 h), and Group 1 composites, 1M(4 h) and 1M(10 h), are shown. It is seen that grains in the non-milled unreinforced alloy, 0AR, are highly elongated in the extrusion direction, reflecting the fibering of the oxide dispersoids during extrusion. In the 4 h-milled unreinforced alloy, 0M(4 h), the elongation of the microstructure is reduced since ball milling leads to an increase in and a more homogeneous distribution of dispersoids [3,12]. For the same milling time the elongated microstructure is less evident in the composite material, 1M(4 h), because large particles disrupt the columnar structure typical of extrusion [6]. Increasing milling time to 10 h, 1M(10 h), produces a more equiaxed microstructure as the quantity of oxide dispersoids and the number of MoSi_2 particles increases.

As is common in FCC extruded alloys [13], the texture of all the materials, comprises two fiber components, namely $\langle 111 \rangle$ deformation texture and $\langle 100 \rangle$ recrystallization texture (with the fiber axis parallel to the extrusion direction), depicted as blue and red respectively, in the maps of Fig. 2. However, the increasing emergence of new orientations when milling time increases is clear from the maps, in particular in the reinforced materials and especially for the group 2 composites. As is well known, the occurrence of discontinuous recrystallization processes based on particle stimulated nucleation (PSN) is widely invoked to explain the microstructure evolution in particle-reinforced metals and texture randomization is one of the distinguishing marks of PSN [14]. According to the theoretical approaches, when the experimental conditions are suitable it gives rise to the creation of new grains, which produces a significant increment of HAB% and decrease in the grain size of the composites in comparison with the monolithic alloy [14]. This can take place when $D_{\text{RF}} > 1 \mu\text{m}$. The present results of particle size after blending, shown in Table 1, suggest that, theoretically,

PSN may only be occurring in the non-milled composites. However, the occurrence of PSN is doubtful because non-milled 1W and 2C composites have roughly the same grain size as the unreinforced non-milled alloy 0AR, even though the composites have many more potential nuclei. Moreover, HAB% is clearly higher in the monolithic alloy. The fact that PSN occurs only to a limited extent can be attributed to the high extrusion temperature [2].

In milled composites, as reinforcing particles are smaller than $1 \mu\text{m}$, a different mechanism must be responsible for texture randomization. Increasing the milling time results in an increase of the volume fraction of oxide dispersoids, of alumina particles, and of small, fragmented intermetallic particles. All these are of small size and therefore contribute strongly to the pinning of grain boundaries, thus preventing both the growth of dynamically recrystallized grains ($\langle 100 \rangle$ red grains) and grain rotation during extrusion (i.e., the formation of the $\langle 111 \rangle$ blue component). Thus, a more random texture is obtained.

4. Conclusions

In this work, EBSD has been used to characterise matrix grain size and grain orientation in six AA6061/ MoSi_2 /15p composites processed with and without ball milling, followed by hot extrusion.

Increasing milling time results in a reduction of matrix grain size to submicrometric level and to a more equiaxed matrix microstructure, mainly due to the increased pinning effect of oxide dispersoids and submicrometric reinforcing particles.

Ball milling favours misorientation and matrix texture randomization in extruded reinforced materials.

Acknowledgement

The authors gratefully acknowledge the financial support of the Spanish project MAT2006-01251. Thanks are also due to Dr M.T. Pérez Prado for helpful discussion.

REFERENCES

- [1] Clyne TW, Withers PJ. An Introduction to Metal Matrix Composites. Cambridge University Press; 1993.
- [2] Borrego A, Fernández R, Cristina MC, Ibáñez J, González-Doncel G. Influence of extrusion temperature on

- the microstructure and the texture of 6061Al-15 vol.%SiCw PM composites. *Comp Sci Technol* 2002;62:731–42.
- [3] Corrochano J, Liebllich M, Ibáñez J. On the role of matrix grain size and particulate reinforcement on the hardness of powder metallurgy Al–Mg–Si/MoSi₂ composites. *Comp Sci Technol* 2009;69:1818–24.
- [4] Parvin N, Assadifard RR, Safarzadeh P, Sheibani S, Marashi P. Preparation and mechanical properties of SiC-reinforced Al6061 composite by mechanical alloying. *Mater Sci Eng* 2008; A492:134–40.
- [5] Kubota M, Cizek P, Rainforth WM. Properties of mechanical milled and spark plasma sintered Al-15 at.% MgB₂ composite materials. *Comp Sci Technol* 2008;66:888–95.
- [6] Jazaeri H, Humphreys FJ. The transition from discontinuous to continuous recrystallization in some aluminium alloys I — the deformed state. *Acta Mater* 2004;52:3239–50.
- [7] Park Young S, Chung Kyung H, Kimb Nack J, Lavernia EJ. Microstructural investigation of nanocrystalline bulk Al–Mg alloy fabricated by cryomilling and extrusion. *Mater Sci Eng A* 2004;374:211–26.
- [8] Angers R, Krishnadev MR, Tremblay R, Corriveau JF, Dubé D. Characterization of SiCp/2024 aluminum alloy composites prepared by mechanical processing in a low energy ball mill. *Mater Sci Eng A* 1999;262(1–2):9–15.
- [9] Fogagnolo JB, Velasco F, Robert MH, Torralba JM. Effect of mechanical alloying on the morphology, microstructure and properties of aluminium matrix composite powders. *Mater Sci Eng A* 2003;342(1–2):131–43.
- [10] Apps PJ, Bowen JR, Prangnell PB. The effect of coarse second-phase particles on the rate of grain refinement during severe deformation processing. *Acta Mater* 2003;51:2811–22.
- [11] Doherty RD, Hughes DA, Humphreys FJ, Jonas JJ, Jull Jensen D, Kassner ME, et al. Current issues in recrystallization: a review. *Mater Sci Eng A* 1997;238:219–74.
- [12] Witkin DB, Lavernia EJ. Synthesis and mechanical behavior of nanostructured materials via cryomilling. *Prog Mater Sci* 2006;5:1–60.
- [13] McHargue CJ, Jetter LK, Ogle JC. Preferred orientation in extruded aluminum rod. *Trans Met Soc AIME* 1959;215:831–7.
- [14] Humphreys FJ, Hatherly M. *Recrystallization and Related Annealing Phenomena*. second ed. Oxford: Elsevier; 2004.